

Seismic Upgrade of Exterior RC Beam-to-Column Joints with CFRP Jacketing: Experimental Investigation



C. Faella, C. Lima, E. Martinelli, A. Napoli & R. Realfonzo

University of Salerno, Italy

J. G. Ruiz Pinilla

Universitat Politècnica de València, ICITECH, Spain

SUMMARY

This paper presents the first results of an experimental campaign performed – at the Laboratory of Materials & Structures of the University of Salerno (Italy) – with the aim to investigate the seismic performance of RC beam-column joints strengthened with FRP and steel systems. The complete test matrix includes eight specimens realized to be representative of existing exterior beam-column subassemblies with inadequate seismic details. Of these, six were strengthened by using different FRP systems while the remaining ones were used as reference benchmark; once damaged, some specimens were also re-tested after being retrofitted with FRP. So far, six tests have been performed of which two were carried out on repaired beam-column joints. The obtained results have allowed to draw some criticisms related to the design of the joint FRP upgrading.

Keywords: beam-column joints, experimental tests, FRP, seismic upgrade

1. INTRODUCTION

Nowadays, repairing and seismic upgrading of underdesigned reinforced concrete (RC) structures represents a key issue in the civil engineering field.

Typically, beam-column assemblages of existing framed buildings were designed to behave in a weak column-strong beam fashion that, under seismic loads, may lead to the formation of local hinges in the column. The associated failure mode represents, therefore, the lower bound of the hierarchy of strength and is characterized by a brittle structural failure.

A number of technical solutions based on the local strengthening of columns have been proposed in the literature with the aim to improve the seismic performance of deficient RC structures. However, in gravity load-designed structures where beams are often stronger than columns, increasing the strength and, mainly, the ductility of columns is generally not sufficient by itself since the joint panel then becomes the next weakest element due to either lack of transverse reinforcement, discontinuous beam bottom reinforcement, or other nonductile detailing.

The brittle failure of joints, significantly reduces the overall ductility of structures and, in some cases, may lead them to the collapse. Therefore, the joint panel should be strengthened by increasing the shear capacity and the effective confinement.

Several repair and strengthening techniques for beam-column joints have been investigated in the literature; they include epoxy repair, removal and replacement of damaged concrete, reinforced or prestressed concrete jacketing, masonry unit jacketing or partial masonry infills, steel jacketing and/or addition of external steel elements, and applications using fiber-reinforced polymer (FRP) materials. Each technique requires a different level of artful detailing and consideration of labor, cost, disruption of building occupancy, and range of applicability. A wide overview on this topic can be found in (Engindeniz et al. 2005).

Within this context, the present paper investigates the feasibility of novel FRP strengthening solutions in increasing the seismic performance of exterior RC beam-column joints. An experimental program was organized at the University of Salerno (Italy) which includes eight specimens representative of existing beam-column subassemblies with inadequate seismic details. Of these, six were strengthened

by using different FRP systems while the remaining ones were used as reference benchmark; once damaged, some specimens were also re-tested after being retrofitted with FRP. So far, six tests have been performed of which two were carried out on repaired beam-column joints. The obtained results have allowed to draw some criticisms related to the design of the joint FRP upgrading.

2. EXPERIMENTAL CAMPAIGN

The ongoing experimental program includes a total of eight RC beam-column joints to subject to reversed cyclic forces applied at the beam tip by keeping the column under a constant axial load; of these, six specimens were strengthened by using different FRP systems while the remaining ones were used as control (unstrengthened) members. After being damaged, some specimens were also repaired, retrofitted with FRP systems and subjected to cyclic tests again. The paper presents the results of the six tests performed up to now, of which two were carried out on FRP retrofitted specimens. The following sections report a detailed description about the design of test specimens, strengthening layouts, test setup and instrumentation.

2.1. Test specimens

Two sets of exterior beam-column joints were designed for the experimental campaign, characterized by different amounts of longitudinal steel reinforcement in the beams and columns. Fig. 1 depicts the geometry and the rebars configuration of the two sets of joints, labeled "Type 1" (Fig. 1a) and "Type 2" (Fig. 1b), respectively, each including four identical specimens. As shown, the columns are the horizontal members having a square 300x300 mm cross section and a length of 2000 mm, whereas the beams are the vertical ones with rectangular 300x400 mm cross section and a length of 1500 mm. In the specimen Type 1, with the aim of simulating the behavior of subassemblies with weak column, the longitudinal steel reinforcement in the beam and column members consists of (3+3) Φ 20 and (2+2) Φ 14 deformed rebars, respectively. Conversely, in the specimen Type 2, in order to obtain the behavior of subassemblies with strong column, a different amount of steel reinforcement ratio was considered, with beam and column reinforced by using (4+4) Φ 20 and (4+4) Φ 14, respectively. The transverse reinforcement in the beam and column members consisted of 8 mm diameter steel stirrups, 100 mm spaced. In order to reproduce subassemblies of RC frames built before the 70's, no steel stirrups were placed in the joints according to the old Italian practice.

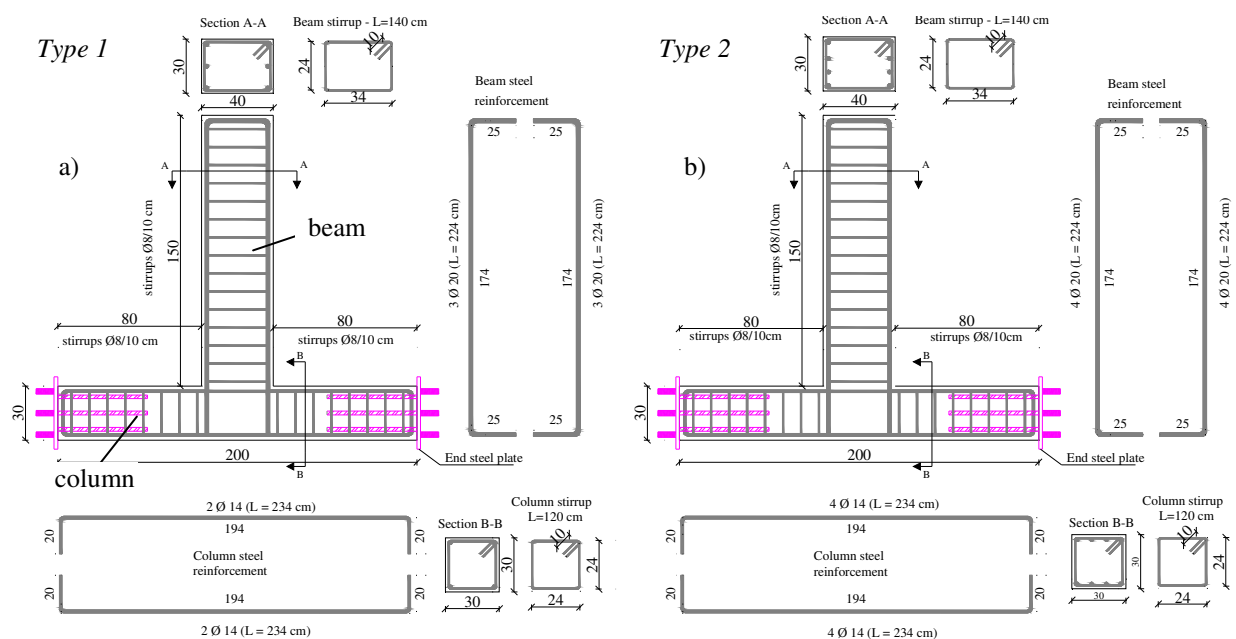


Figure 1. Geometry and steel reinforcement configuration for specimens Type 1 (a) and Type 2 (b).

Table 1 reports the mechanical properties used for specimen design, being: f_y and E_s the average values of the yielding strength and elastic modulus of steel rebars, respectively; f_c and E_c the respective values of the compression strength and elasticity modulus of concrete, $\lambda = 1.20$ is the steel overstrength factor.

Table 1. Mechanical properties of test specimens.

column		beam			joint		E_s	E_c
f_y	f_c	f_y	f_c	λ	f_y	f_c		
(MPa)	(MPa)	(MPa)	(MPa)	[-]	(MPa)	(MPa)	(MPa)	(MPa)
540	16	540	16	1.20	540	16	210000	28750

The design of specimens was performed with the aim to achieve the connection failure having the column weaker than the beam but always stronger than the joint panel. To this purpose, five capacity models were selected from the literature and codes provisions in order to estimate the joint shear strength $V_{R,jh}$, i.e. the models by: Italian Code (NTC 2008) for evaluating the strength of joints belonging to new structures (*model 1a*) or assessing those of existing ones (*model 1b*); Paulay & Priestley (1992) (*model 2*); Vollum & Newman (1999) (*model 3*); Bakir & Boduroglu (2002) (*model 4*); Kim et al. (2009) (*model 5*). A wide overview of all joint strength models proposed in the literature, omitted herein for the sake of brevity, can be found in Lima et al. (2012).

Table 2 reports the values of shear strength $V_{R,jh}$ estimated for the two joints types according to the five models, by assuming a constant axial load in the column equal to 300 kN.

Table 2. Estimated values of the joint shear strength $V_{R,jh}$ [kN].

TYPE	Model 1a	Model 1b	Model 2	Model 3	Model 4	Model 5
1	210.84	174.60	323.15	320.57	204.80	290.60
2	208.48	173.30	360.00	316.63	228.86	313.30

By considering the testing configuration depicted in Figure 2a, the experimental value of the joint shear force V_{jh}^{exp} , relying on the force P^{exp} applied by the actuator at the beam tip, can be easily evaluated by equilibrium throughout the joint panel (see Fig. 2b):

$$V_{jh}^{exp} = \frac{P^{exp} \cdot L_b}{M_y} A_{s,b} \cdot f_{y,b} - \frac{P^{exp} \cdot L_b}{2L_c} = T^{exp} - V_c^{exp} \quad (2.1)$$

where: V_c^{exp} is the shear force in the column, T^{exp} is the force of the top rebars in the beam, $A_{s,b}$ is the area of the beam steel reinforcement in tension; the lengths L_b and L_c indicated in Fig. 2a are equal to 1580 and 1300 mm, respectively.

In Eqn. 2.1 it has been assumed that the joint panel failure occurs before the beam yielding (according to the design criteria), i.e. the experimental bending moment acting on the joint at peak ($M^{exp} = P^{exp} \cdot L_b$) is lower than the value at yielding of the beam (M_y).

By plugging $V_{jh}^{exp} = V_{R,jh}$, the ultimate value of P^{exp} can be finally derived from Eqn. 2.1 and the results obtained from considering the five strength models are reported in Table 3.

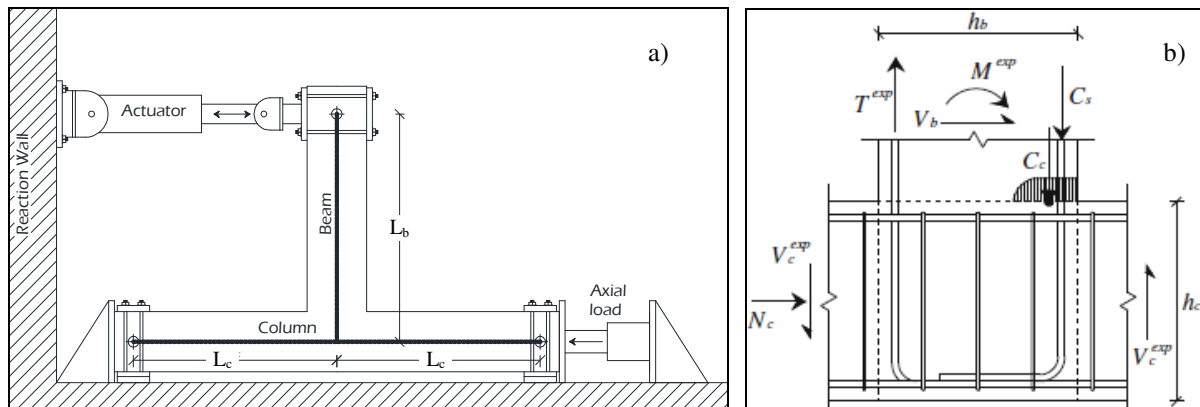


Figure 2. Test configuration for exterior joints (a); equilibrium throughout the joint panel (b).

Table 3. Estimated values of the ultimate actuator load P^{exp} (kN).

TYPE	Model 1a	Model 1b	Model 2	Model 3	Model 4	Model 5
1	44.86	37.15	49.39	68.20	43.57	61.83
2	44.03	36.60	76.03	66.87	48.33	66.16

2.2. FRP layouts for upgrading and retrofitting of specimens

2.2.1. Strengthened specimens

Fig. 3 depicts the three upgrading schemes adopted for the first tested "Type 1" beam-column joints, labeled J-02 (Fig. 3a), J-03 (Fig. 3b) and J-04 (Fig. 3c). The strengthening design was based on the following two principles: a) upgrading the joint panel without causing a premature failure of the column during test; b) achieving the most desirable collapse mechanism, i.e. the beam failure.

In order to pursue these objectives, both columns and joints panels were strengthened.

In all the three schemes, the column upgrading consisted of longitudinal cold bent steel profiles along the member corners before applying the external continuous wrapping made of two carbon FRP (CFRP) layers. The profiles were four 80x80x6 mm equal leg angles made of structural steel S235; they were always glued to the concrete substrate by means of an epoxy adhesive. In the schemes J-02 and J-03, the profiles were always interrupted at the beam-column intersection; in the scheme J-04, instead, such angles were continuous on the exterior face of the joint and discontinuous at the beam-column intersection, thus providing the joint panel with a better confinement.

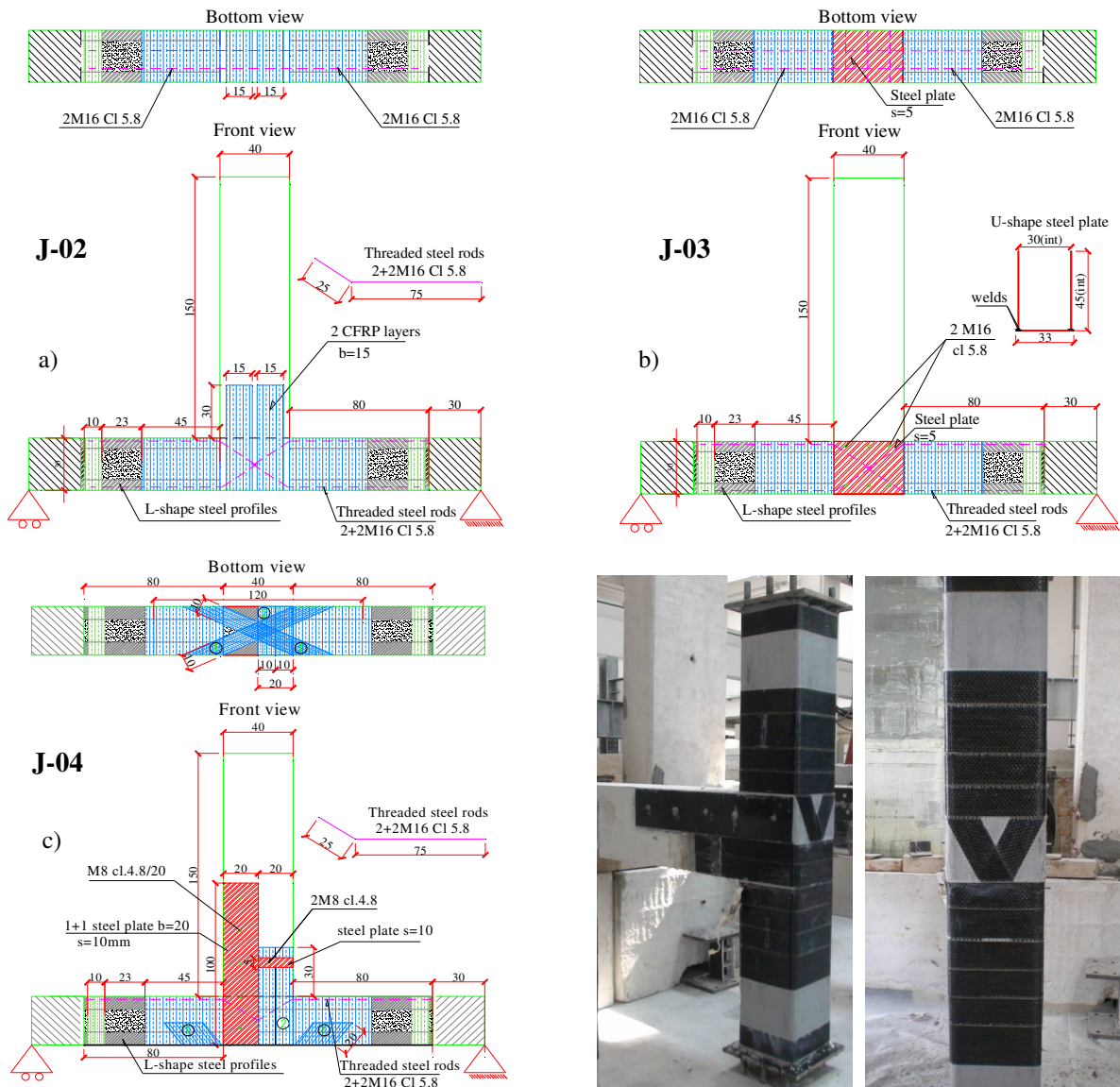


Figure 3. Strengthening layouts for specimens J-02 (a), J-03 (b) and J-04 (c).

In order to increase the flexural strength of the columns, $(2+2)\Phi 16$ threaded rods were glued with epoxy within the concrete cover and anchored in the joint panel.

The employed CFRP plies, each 0.22 mm thick, were characterized by an elastic modulus of 390 GPa, a tensile strength of 3000 MPa and an ultimate strain equal to 0.80 %.

In the case of the specimen J-02, according to a frequently used retrofitting system, the joint panel was strengthened by employing two U-shape CFRP-layers, 150 mm wide, which were anchored on the beam for a length of about 300 mm.

In order to simulate the behavior of an exterior RC joint with three high RC beams (i.e. a "well confined" joint), the joint of the specimen J-03 was strengthened by using a U-shape steel plate, 5 mm thick, properly anchored with threaded rods (with 16 mm diameter) through the joint. This layout may represent the target configuration for strength and stiffness related to out-of plane behavior.

In the case of the specimen J-04, instead, the joint panel was strengthened with the aim to address issues raised from the test performed on the specimen J-02. First of all, as shown in Fig. 3c, two steel plates, 200 mm width and 100 mm thick were placed with the purpose to simulate, in a simplified manner, the presence of a floor slab contributing to confine the joint panel in the directions orthogonal to the axis of the beam represented in the figure. Also, as better shown in the picture on the right, the exterior face of the joint panel was strengthened with cross CFRP sheets, 100 mm wide, which were restrained within the column external wrapping. Finally, the joint panel was further strengthened, in the region close to the steel plates, by employing two U-shape CFRP-layers, 100 mm wide, which were anchored on the beam for a length of about 300 mm. Unlike the scheme J-02, a mechanical anchorage of these CFRP sheets was used in order to avoid a premature FRP debonding.

2.2.2. Repaired and retrofitted specimens

As mentioned earlier, some specimens, after being damaged, were repaired, retrofitted with FRP systems and subjected to cyclic tests again. This is the case of specimens J-01 (originally unstrengthened and used as a reference member) and J-02 that were repaired and retrofitted according to the schemes J-01_R (Fig. 4a) and J-02_R (Fig. 4b), respectively. In particular, the scheme J-01_R is very similar to the scheme J-04 but the column retrofit was performed by using CFRP wrapping w/o steel profiles and threaded rods. The scheme J-02_R, instead, is characterized by the use of two layers of longitudinal CFRP sheets, 100 wide, as a replacement of the cross one employed in the schemes J-04 and J-01_R; the column retrofit, instead, is that originally used for the specimens J-02.

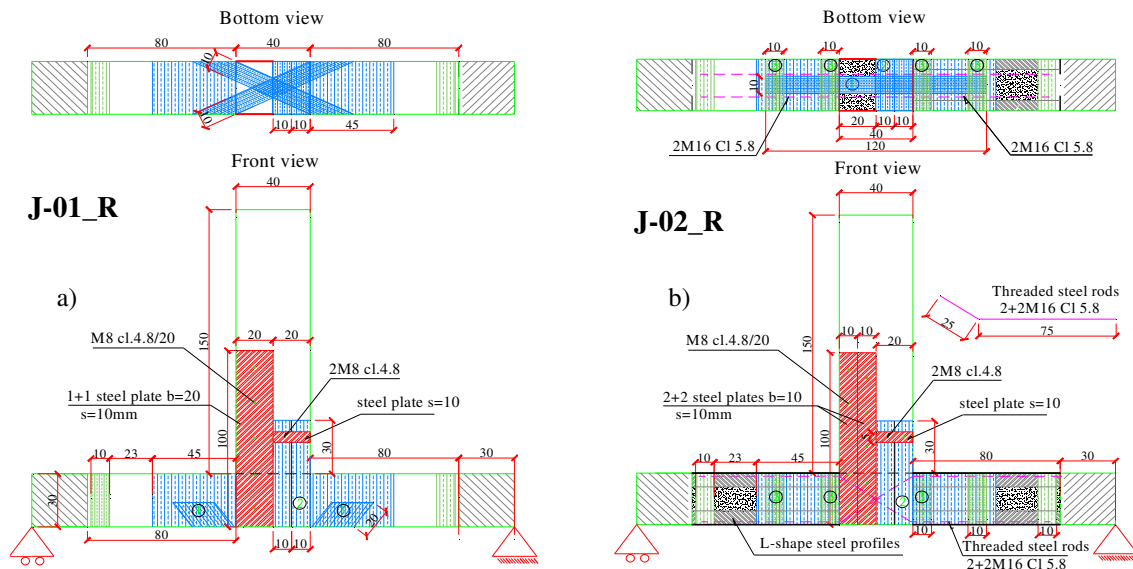


Figure 4. Retrofit schemes for specimens J-01_R (a) and J-02_R (b).

2.3. Test set-up

Fig. 5a shows the set-up adopted for subjecting the beam-column joints to reversed cyclic forces applied at the beam tip by keeping the column under a constant axial load. The column was mounted

horizontally and restrained to both ends by assembling steel elements according to a roller-hinged scheme. It was pre-loaded in compression before applying the horizontal force by using a 1000 kN MTS hydraulic actuator fixed to a reaction steel frame. The axial load N , kept constant during the test, was equal to about 300 kN, corresponding to a normalized compression load "v" of ≈ 0.20 , given by:

$$v = \frac{N}{f_{cm} \cdot A_g} \quad (2.2)$$

where A_g is the column cross-section and f_{cm} is the average value of the cylinder compressive strength of concrete. The latter was obtained from the relationship $f_{cm} = 0.83 R_{cm}$, where R_{cm} was estimated by testing in compression cubic 150-mm side specimens, taken during the casting of each column and cured under the same environmental conditions.

The horizontal force was cyclically applied in displacement control at the beam tip through a 250 kN MTS hydraulic actuator, mounted at 1430 mm from the beam base and fixed to a reaction steel frame. The time history of the horizontal displacement is shown in Fig. 5b. An increment of the imposed horizontal displacement every three cycles was considered in order to evaluate the strength and stiffness degradation at repeated lateral load reversals. The displacement amplitude increment was given as fraction of the estimated beam yield displacement, Δy (≈ 14 mm); two different displacement rates were considered during the tests: 0.2 mm/s before the achievement of Δy and 1 mm/s after Δy . The joint panels were accurately instrumented in order to monitor strains, displacements and crack widths. An accurate description on the considered instrumentation can be found in Faella et al (2012).

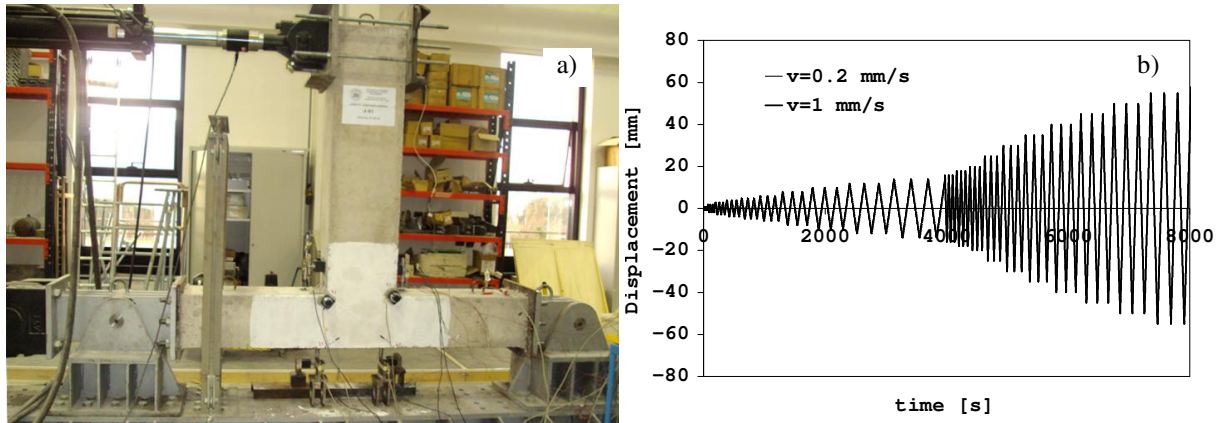


Figure 5. Test set-up (a); displacement history (b).

3. TEST RESULTS AND DISCUSSION

Table 4 summarizes the main results of the six tests performed so far. In particular, the label J-01 identifies the control (unstrengthened) specimen, while J-02, J-03 and J-04 are relative to specimens upgraded according to the FRP layouts shown in Fig. 3. The labels J-01_R and J-02_R, instead, identify the specimens J-01 and J-02, respectively, that once being damaged, were repaired and FRP retrofitted according to the schemes illustrated in Fig. 4.

In Table 4: f_{cm} is the average value of the cylinder compressive strength of concrete; v is the normalized value of the axial load N ; F_{max}^+ and F_{min}^- are the peak lateral strengths in the two directions of loading, whereas Δ^+ and Δ^- are the corresponding displacements, $\Delta_{85\%}^+$ and $\Delta_{85\%}^-$ are the maximum displacements exhibited at the conventional collapse (i.e. at the achievement of 15% strength degradation evaluated on the lateral force-displacement envelopes). The last column of the table describes the failure modes experienced by specimens at collapse.

As evidenced in the following sections, the obtained results have provided useful information about the efficacy of the retrofitting/upgrading schemes considered in the preliminary phase of the experimental campaign.

Table 4. Test results and failure modes.

Test	FRP layout	f_{cm} (MPa)	ν	F_{max}^+ (KN)	F_{max}^- (KN)	Δ^+ (mm)	Δ^- (mm)	$\Delta_{85\%}^+$ (mm)	$\Delta_{85\%}^-$ (mm)	Failure mode
J-01	/	16.4	0.20	62.5	-66.1	16	-10	25.9	-21.1	Joint shear failure
J-02	Fig. 3a	19.5	0.17	67.6	-80.7	18	-14	27.7	-24.2	FRP delamination followed by joint shear failure
J-03	Fig. 3b	15.7	0.21	118.8	-90.3	30	-30	49.2	-45.5	Flexural beam failure
J-04	Fig. 3c	19.0	0.17	130.3	-91.3	30	-30	51.1	-41.8	slight FRP delamination followed by flexural beam failure
J-01_R	Fig. 4a	16.4	0.20	61.5	-66.0	30	-30	46.6	-44.5	slight FRP delamination followed by joint shear failure
J-02_R	Fig. 4b	19.5	0.17	84.5	-75.8	25	-30	35.6	-33.5	slight FRP delamination followed by joint shear failure

3.1. Cyclic behaviour

3.1.1. FRP strengthened specimens

By comparing the results reported in Table 4, it is observed that the specimen J-02, having the joint panel upgraded with two "U"-shape CFRP sheets, has shown results only slightly better than those of the unstrengthened member J-01. This reduced performance, both in terms of strength and ductility, lies in the premature achievement of the conventional collapse by FRP intermediate debonding. Conversely, significant increases of strength and ductility were obtained in the case of the tests J-03 and J-04 where the selected strengthening systems better preserved the joint panel integrity. On the average, the specimen J-03 provided an increase of strength and ductility over the member J-01 equal to about 63% and 100%, respectively; for the member J-04, instead, the corresponding percentage increases were 72% (for the strength) and 98% (for the ductility). In both cases, the improved performance of the joint, combined with an effective strengthening of the column, allowed to move the failure in the beam, which represents the upper bound of the hierarchy of strength.

In Fig. 6a, the lateral load (F)-displacement (Δ) cyclic curves for the specimens J-03 and J-04 are compared with that of the control member J-01; in Fig. 6b, instead, the F- Δ envelopes for the four tests are plotted. The comparisons better highlight the beneficial effects obtained from the tests J-03/04 and the rather identical behavior observed for the specimens J-01 and J-02.

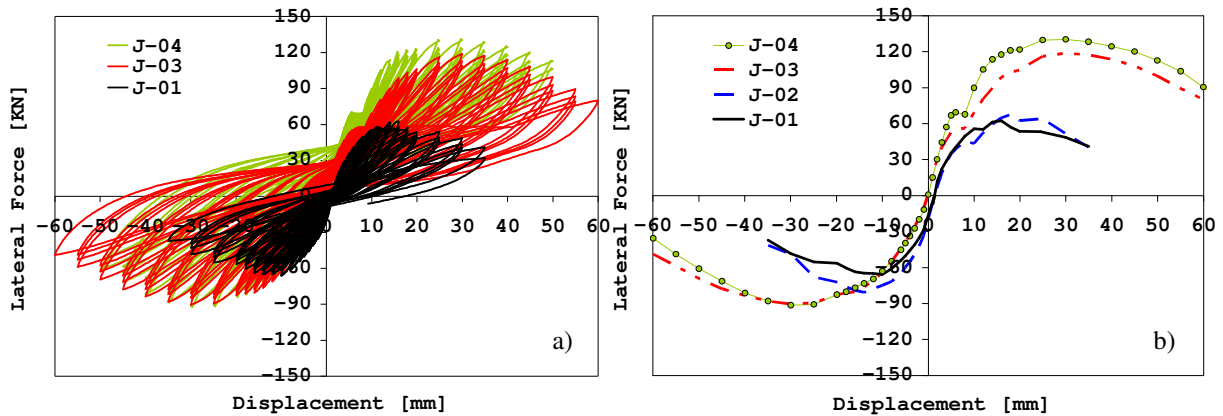


Figure 6. Load-displacement curves: a) hysteresis loops; b) envelopes.

3.1.2. Repaired and FRP retrofitted specimens

The considered FRP retrofitted systems have allowed to restore and in some cases improve the cyclic response of the "original" specimens. From Table 4 it is observed that the retrofitted specimen J-01_R has exhibited a behavior significantly more ductile than the counterpart J-01 (ductility almost doubled), while the strengths are comparable. For the specimen J-02_R, a slight strength increase over the "original" member J-02 is also observed. The effectiveness of the selected retrofit schemes is clearly visible from Fig. 7 where the comparisons in terms of F- Δ cyclic curves are reported for specimens J-01/J-01_R and J-02/J-02_R. In Fig. 8, instead, the F- Δ envelopes are plotted. It is noted a substantially identical behaviour in terms of strength between "original" and retrofitted members, and a greater ductility for FRP retrofitted members. As expected, the F- Δ envelopes relative to retrofitted members exhibit an initial stiffness lower than that of the corresponding members J-01 and J-02.

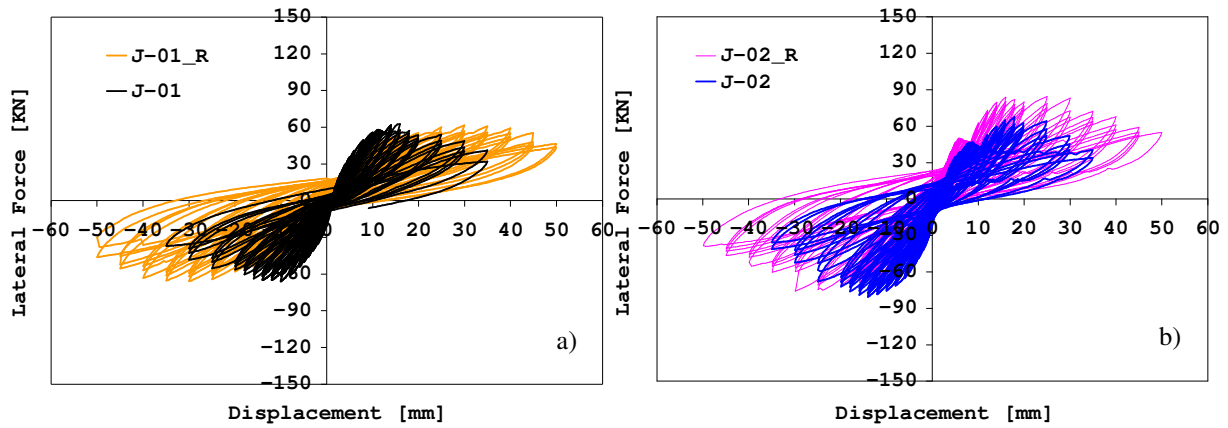


Figure 7. Comparisons between upgraded and retrofitted specimens: load-displacement curves

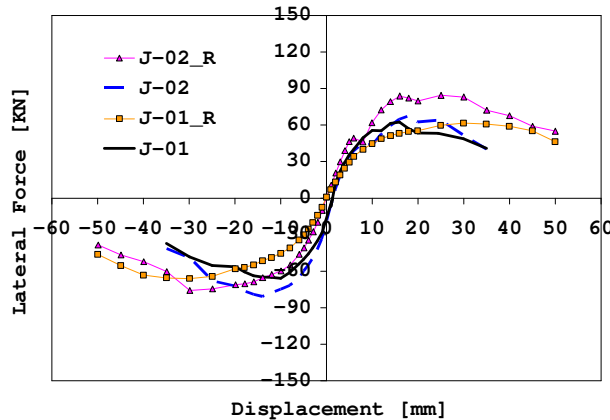


Figure 8. Comparisons between upgraded and retrofitted specimens: F- Δ envelopes.

3.2. Failure mode

Fig. 9 shows the scenario of damage exhibited by specimens at the end of tests.

The control specimen J-01 highlighted a significant vulnerability of the joint panel region. The first signs of damage occurred at the beam-column interface during an imposed displacement of 5 mm; they consisted of small flexural cracks whose width did not significantly increase during the test. Then, several shear cracks start to develop in the joint region but these did not affect the member strength up to a displacement of 20 mm, i.e. when the cracks along the four diagonal of the panel became dominant. In this test, the collapse was characterized by spalling of the concrete outer wedge which left the anchorage of the beam longitudinal reinforcement discovered (Fig. 9a).

As mentioned in the previous section, the behavior of the specimen J-02 was strongly influenced by the premature delamination of the FRP layers which were not well anchored on the beam face by proper anchorage systems. This phenomenon was induced by the opening of flexural cracks at the beam-column interface during a displacement value of 10 mm. The damage was then followed by the development of relevant vertical cracks which, starting from the beam-column interface, propagated along the beam parallel to the FRP sheets. In absence of joint confinement, the failure of the specimen was carried out in the same way as J-01 (Fig. 9b).

The specimen J-03 exhibited a different response with respect to the other members. The joint strengthening was able to significantly improve the cyclic behavior of the joint panel by moving the rupture of the specimen to the beam. In this case, the strength of the specimen was controlled by the maximum flexural capacity of the beam. As shown in Fig. 9c, the damage was characterized by a large flexural crack concentrated at the beam-joint interface.

The specimen J-04 has experienced a significantly improved behavior with respect to the member J-02. The use of continuous steel profiles and cross FRP sheets on the exterior joint face assured a better confinement of the panel region, thus delaying the spalling of the concrete outer wedge. In this case, the debonding of the FRP first occurred only at the sheet end above the anchorage system and then,

propagated in other portions of the FRP; however, at collapse the sheet was still firmly attached on the beam through the used anchorage systems (Fig. 9d). During the test, a slight rotation of the steel plates simulating the presence of a floor caused a local damage of the FRP regions in contact with them. The damage behavior of retrofitted specimens was quite similar to that of the specimens J-04. However, in the case of the specimen J-01_R the lack of adequate confinement assured by the use of steel profiles caused a significant damage of the joint panel (Fig. 9e).

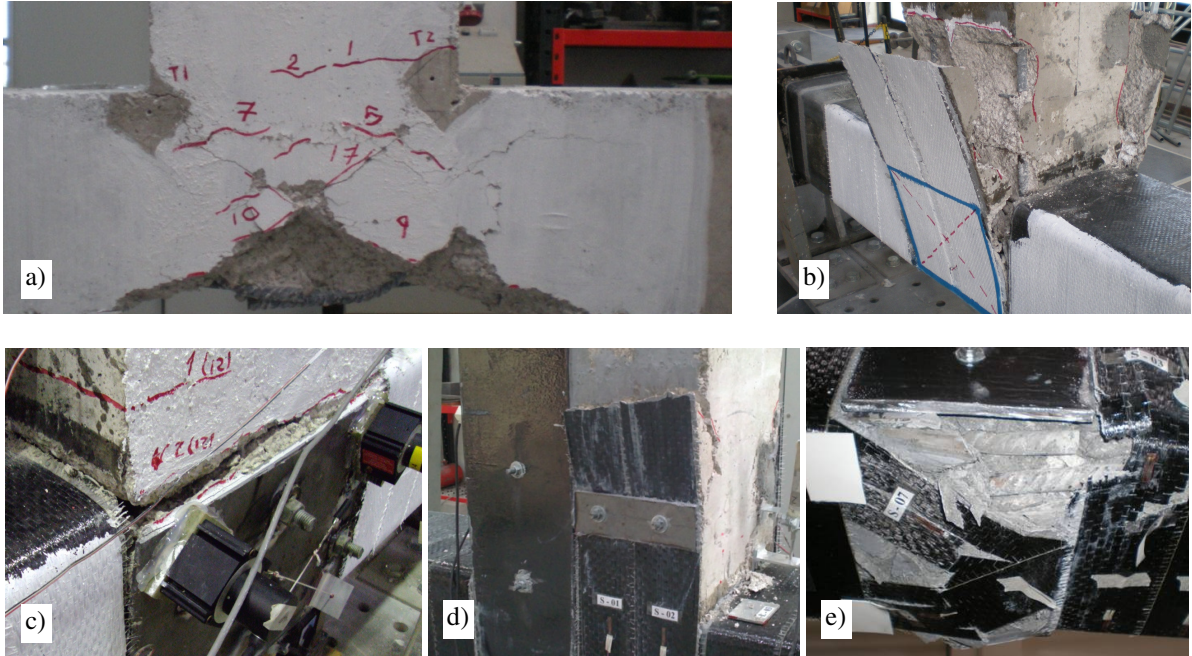


Figure 9. Damage pattern of specimens: J-01 (a); J-02 (b); J-03 (c); J-04 (d) and J-01_R (e).

3.3. Stiffness degradation and energy dissipation

Based on the experimental results, it was possible to evaluate the mean value of stiffness for the i th cycle by using the following ratio (Mayes and Clough 1975):

$$k = \frac{|F_{max,i}^+| + |F_{max,i}^-|}{|\Delta_{max,i}^+| + |\Delta_{max,i}^-|} \quad (3.1)$$

The stiffness of each cycle was then normalized with respect to the stiffness of the first cycle K_1 , thus providing a measure of the stiffness degradation.

The relationship between the K/K_1 ratio and the imposed displacement is plotted in Fig. 10a for all tested specimens. As shown, the stiffness degradation is quite similar for specimens approximately up to a displacement value of 10 mm, i.e. when all the joint panels still exhibit a negligible state of damage. After this threshold, a greater stiffness decrease was evaluated for the specimens J-01 and J-02, as the progressive propagation of damage caused an abrupt reduction of the joint strength. For the other members, instead, the relationship between the K/K_1 ratio and the displacement is rather independent on the type of FRP strengthening technique.

Finally, Fig. 10b depicts the relationships between the cumulative dissipated energy (E) and the imposed beam displacement; this energy parameter was calculated – at each imposed displacement – from the area under the $F-\Delta$ response enclosed within one complete cycle. As observed for the stiffness, the energy computed up to the displacement cycle of 10 mm is approximately the same for all tests. However, the cumulative dissipated energy is considerably higher in the case of the specimen J-03 and J-04, as the techniques adopted for joint strengthening produced a significant increase of ductility. It is also worth noting that the retrofitted specimens J-01_R and J-02_R are able to dissipate approximately the same energy amount of the corresponding strengthened members J-01 and J-02.

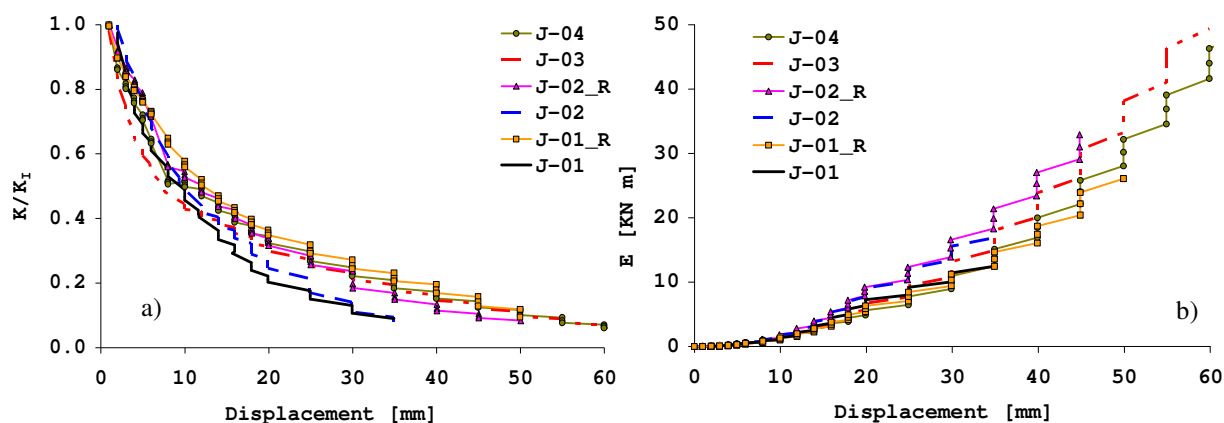


Figure 10. Stiffness degradation (a); Total dissipated energy (b).

4. CONCLUSIONS

In this paper, the first results of cyclic tests carried out on exterior RC beam-column joints have been discussed. Four assemblies have been tested, i.e.: a benchmark (unstrengthened) specimen, used as comparison term, and three upgraded specimens characterized by the strengthening of both column and joint members. After being damaged, two of these assemblies were also repaired, retrofitted with FRP systems and subjected to cyclic tests again. The performed tests have highlighted some critical aspects related to a poor design of the joint FRP upgrading. In particular, due to intermediate debonding, the joint panel strengthened with FRP sheets not well anchored by proper mechanical anchorage showed only a slightly better behavior than that of the unstrengthened one. Conversely, by improving the strengthening design, the joint upgrading with FRP systems allowed to move the failure in the beam, in full conformity with the hierarchy of strength. Finally, tests performed on FRP retrofitted members have allowed to restore the strength and significantly increase the ductility of the "original" members.

ACKNOWLEDGEMENT

The Authors gratefully acknowledge "F.lli Abagnale sas" precasting company (Naples, Italy) for concrete specimens production, and "Interbau srl" (Milan, Italy) for the financial support to the experimental program and the realization of the FRP strengthening systems.

REFERENCES

- Bakir, P.G. and Boduroglu, H.M. (2002). A New Design Equation for Predicting the Joint Shear Strength of Monotonically Loaded Exterior Beam-To-Column Joints. *Engineering Structures*, **24**, 1105-1117.
- Decreto Ministeriale 14 Gennaio 2008, "Norme Tecniche per le Costruzioni", GU. N.29 del 4 Febbraio 2008 (in italian).
- Engindeniz, M., Kahn, L.F. and Zureick, A.H. (2005). Repair and Strengthening of Reinforced Concrete Beam-Column Joints: State of the Art. *ACI Structural Journal* **102:2**, 1-14.
- Kim, J., La Fave, J.M. and Song J. (2009). Joint Shear Behaviour of Reinforced Concrete Beam-Column Connections. *Magazine of Concrete Research*, **61:2**, 119-132.
- Lima, C., Martinelli, E. and Faella, C. (2012). Capacity Models for Shear Strength of Exterior Joints in RC Frames: State-Of-The-Art And Synoptic Examination. *Bulletin Of Earthquake Engineering*, (in printing) DOI: 10.1007/S10518-012-9340-4.
- Mayes, R.L. and Clough, R.W. (1975). State of the Art in Seismic Shear Strength of Masonry – An Evaluation And Review. Eerc Report, Berkeley, California, USA.
- Paulay, T. and Priestley, M.J.N. (1992). Seismic Design Of Reinforced Concrete And Masonry Buildings. John Wiley & Sons Eds., NY, USA.
- Vollum, R.L. and Newman, J.B. (1999). The Design of External, Reinforced Concrete Beam Column Joints. *The Structural Engineer* **77:23**, 21-27.
- Faella, C., Lima, C., Napoli, A., Realfonzo, R. and Ruiz Pinilla, J.G. (2012). Beam-Column Joints Strengthened with FRP Systems. Submitted for publication to *Proceedings of CICE 2012*, Rome, June 13-15